Influence of Shoulder Hemiarthroplasty Protocol on the Nature of the Glenoid Tissues at the Hemi-Implant Interface: A Three Cases Study Case Series

Rémy Gauthier, Amira Hanoun, Nina Attik, Michel Hassler, Ana-Maria Trunfio-Sfarghiu

Influence of shoulder hemiarthroplasty protocol on the nature of the glenoid tissues at the hemi-implant interface: a three cases study

Rémy Gauthier[1*]; Amira Hanoun[2,3] ; Nina Attik[4,5]; Michel Hassler[3] ; Ana-Maria Trunfio-Sfarghiu[2]

[1]Univ Lyon, CNRS, INSA Lyon, Université Claude Bernard Lyon 1, UMR 5510, MATEIS, F-69621 Villeurbanne, France.

[2]Univ Lyon, INSA Lyon, CNRS UMR5259, LaMCoS, Villeurbanne F-69621, France.

[3]Tornier SAS, Grenoble, France

[4]Univ Lyon, Université Claude Bernard Lyon 1, UMR CNRS 5615, Laboratoire des Multimatériaux et Interfaces, F-69622 Villeurbanne, France.

[5]Univ Lyon, Université Claude Bernard Lyon 1, Faculté d'Odontologie, 69008 Lyon, France.

Abstract: The interactions between a hemi-implant head and the native glenoid cavity are determinant in the efficiency and longevity of the medical strategy. The glenoid tissues harvested from three clinical cases who underwent different types of shoulder hemi-arthroplasty were investigated. A first case with a cobalt- chrome (CoCr) head presented a loose and multi-layered fibrocartilaginous tissue with CoCr particles and areas of inflammation. The bone marrow was hypercellular and fibrous, highlighting the inflammatory state of the joint. The second case with a pyrocarbon (PyC) head presented a glenoid membrane made of articular cartilage and fibrocellular tissue with collagen II expression. The third case with a PyC head and subchondral microdrills presented the tissue with the best quality. The glenoid membrane was mainly composed of articular cartilaginous like tissue and the bone marrow presented a normal morphology, with some expression of collagen II on the vascular walls. A lipidomic analysis showed that the PyC had a better capacity to adsorbed a layer of lipids on its surface compared to the CoCr. The amount of lipids was enhanced in the case of subchondral microdrills, probably due to the liberation of the bone marrow lipids. As it is known for the healthy cartilage, a lipids layer improves the biomechanical interaction occurring at the implant-glenoid cavity interface in favour of decreased frictional forces and an enhanced joint integrity. Despite the limitations of the current study, these results strongly support for further investigations of the PyC-glenoid tissues interactions.

Keywords: Shoulder hemiarthroplasty; Tissue implant interaction; Mechanobiology; Tribology; Lipids Layer.

1. Introduction

Healing shoulder joints remains a clinical, scientific, and societal challenge. Total Shoulder Arthroplasty (TSA) or hemi-arthroplasty (HA) represent the main current healing surgeries to replace a wounded shoulder. TSA presents good short-terms clinical outcomes clinical, but shows an increasing risk for the glenoid component failure after mid-terms follow-up on young patients (Matsen et al., 2008; Papadonikolakis et al., 2013). HA is a more conservative surgery procedure that saves the patient native glenoid cavity. Still, a 17-years follow up clinical study showed that 75 % of the patients who underwent a HA did suffer from pain due to glenoid erosion (Levine et al., 2012). Glenoid erosion is characterised by a loss of glenoid bone stock. Clinically, it is generally explained by the degeneration of the cartilage and the wear of the underlying bone due to detrimental tissue-implant frictions. Current hemi-implants are mainly made of cobalt chrome (CoCr), that is known to have bad wear outcomes against cartilage compared to other biomaterials (Chan et al., 2011; Klawitter et al., 2020; Vanlommel et al., 2017). Recently, hemi-implants with a pyrocarbon (or pyrolytic carbon, PyC) head have shown interesting short-terms and mid-terms outcomes (Franceschetti et al., 2023; Garret et al., 2019). PyC is known to

have enhanced wear characteristics compared to CoCr (Impergre et al., 2023; Klawitter et al., 2020), what can partly explain a lower glenoid erosion rate (McBride et al., 2021).

The joint biomechanics is of great importance in its integrity. Bone and cartilage are both biologically sensitive to the applied mechanical loading. More particularly, it is assumed that the mechanical fatigue-induced bone remodeling is involved in cartilage degeneration (Coughlin and Kennedy, 2016; Zarka et al., 2019). It is also known that the subchondral bone marrow stimulation influences the cartilage integrity. Marrow stem cells from have a chondrogenic capacity (Elder et al., 2009) and bone marrow lesions due to an abnormal loading have been associated with cartilage degeneration (Alliston et al., 2018). Monitoring the mechanical loading transmitted to the bone is thus determinant in the regulation of the cartilage layer.

In regard of this bone-cartilage cross talk, a method consisting in drilling microholes in the subchondral plate to promote bone-cartilage communication was developed for the treatment of osteoarthritic joint (Martin and Jakob, 2022). This microdrilling is assumed to liberate stem cells and other elements from the underlying bone marrow thus promoting new cartilage formation (Broyles et al., 2017).

Interestingly, phospholipids (PL) are assumed to play a major role in cartilage surface lubrication. by being adsorbed on the cartilage PL increases the surface hydrophobicity thus limiting its interactions with other tissues (Hills, 2002). Furthermore, the amount of PL on osteoarthritic cartilage surface is decreased together with its hydrophobicity (Hills, 2002). The increased interactions between the cartilage with an increased hydrophilicity with surrounding tissues partly explain its degeneration. Promoting the formation of a lubricant layer at the glenoid implant interface may thus be a relevant way to decrease tissue-implant mechanical frictions and the development of durable treatments. Interestingly, bone marrow is known to contain phospholipids (During et al., 2015).

In that context, the current study aim was to investigate the differences in the nature of human glenoid tissues in contact with hemi-implant heads in different HA configurations. These tissues were harvested from three HA clinical cases: a CrCo hemi-implant head (CrCo), a PyC hemi-implant head (PyC), and a PyC hemi-implant head with subchondral microdrilling (µPyC). The tissues were investigated through histological and lipidomic analyses.

2. Materials and methods

2.1. Cohort

The cohort consisted in 3 patients who underwent a revision surgery after a HA between 2016 and 2021 by three different surgeons. The tissue samples were recovered with the patients and the surgeons' consent.

- Case 1: CrCo head (CrCo):

This patient was a 60 y.o. man at the time of the HA revision. He had a previous surgery consisting of staples implantation to stabilize the joint (unknown date of surgery). On March 2015, he underwent a CrCo HA surgery because of abnormal pain and osteoarthritis of the joint. Because of the glenoid erosion against the metallic head, the patient suffered from pain and underwent a revision surgery after 21 months (December 2016). The surgeons diagnosed that due to the misplacement of the implant, osteophytes appeared without glenoid deviation. The HA was then converted in a total reversed shoulder arthroplasty.

- Case 2: PyC head (PyC)

This patient was a 59 y.o. man at the time of the HA revision. The PyC head was implanted in November 2018 and revised 31 months after (June 2021) due to pain. The surgeons did not identify accurately the link between the device and the pain. After head removal, the surgeon noticed a glenoid cartilage in

good status. The hypothesis was that the implant stem was oversized. The HA was converted in to total shoulder arthroplasty.

- Case 3: PyC hemi-implant with microdrilling (µPyC)

This patient was a 67 y.o woman at the time of the HA revision. In 1991, she suffered from a traumatic humeral head fracture and was treated using plate osteosynthesis to treat tuberosity fractures. In September 2015, she underwent a HA using a PyC head because of pain and high glenoid erosion due to traumatic osteoarthritis. Microdrilling were performed by the surgeon on the areas lacking cartilage. the µPyC HA was revised 15 months later (January 2017) due to abnormal pain. The surgeon declared that the patient presented a malunion after the humeral head trauma making it difficult to place the hemi-implant stem properly. In consequence, the stem was lateralized, generating abnormal hypertension in the joint.

2.2. Tissue removal

The investigated tissues were harvested directly by the surgeons at the time of the HA revision. It was told to the surgeons to harvest both a part of the glenoid cartilage membrane and a bone core (Figure 1). For the PyC case (case 2), the surgeons harvested a bone-cartilage core. The tissues were then stored in AFA (Alcool-Formol-Acetic Acid) until preparation for histological analyses.

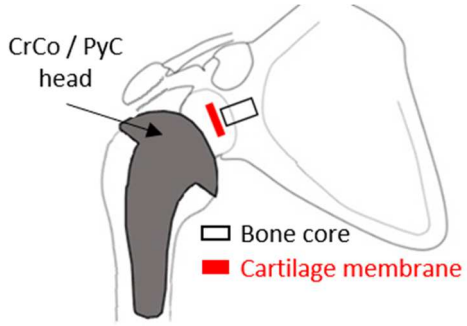

Figure 1: Schematic of the implanted shoulder illustrating the harvesting tissues. 1 column fitting image

2.3. Tissue analysis

Samples were fixed in 4 v% formalin, embedded in paraffin, and 5 µm sections were cut. Mineralized tissues were decalcified before cutting. Hematoxylin, Eosin, Safran (HES) staining was then applied on different sections. HES stains cells nuclei in purples, cells cytoplasm in pin and extracellular matrix in yellow.

Additionally, immunochemical stainings were applied to analyse the expression of collagen I (Coll I) and collagen II (Coll II) in the samples. After removing the paraffin, the samples were immerged in 0.5 % hyaluronidase buffered in PBS-BSA 3% for 1h at room temperature in order to expose the antigenic sites. Sections were then incubated with rabbit anti-human Coll I diluted at 1/1000 (20111, Novotec, France) and rabbit anti-human Coll II diluted at 1/500 (20211, Novotec, France) overnight at 4°C buffered in PBS-BSA 3%. Samples were then incubated with goat anti-rabbit secondary anti-body coupled with peroxidase (K4002, Envison Lapin, Dako, USA). A final reaction with diaminobenzidine (K36008, Dako, USA) revealed the antigenic – antibody complexes through a brown color. All the samples were analysed by Novotec (Lyon, France) except from the HES of the PyC case that was analyse by the Ciqle platform (Lyon, France).

2.4. Lipidomic analysis

The CrCo and PyC explanted heads were first washed with saline solution to remove traces of blood. A solution of ethanol and chloroform (1:2, v:v) was then used to wash twice the heads and extract the lipids. The solutions were then stored at – 20°C until analysis. Before the analysis, the samples were dried and diluted in 100 µL of the same solvent (ethanol: chloroform, 1:2). Lipids were separated through thin-layer chromatography. In brief, 90 µL of the solution were deposited on a thin-layer chromatography plate silica gel (60 F254, Merck). The migration occurred in a mixture of n-hexane, diethyl ether, and acetic acid (80:25:1, v:v:v) for 90 minutes. Samples were then dried under dry nitrogen; migration spots were visualized under UV lamp at 254 nm and compared with standards. The identified phospholipids (PL) were then collected and diluted in a solution of 1 mL of methanol and toluene (1:1, v:v) and 500 µl of 14% boron-trifluoride in methanol. The solutions were then heated at 100 °C for 90 minutes to allow for transesterification that separates the fatty acids from the lipid heads.

The fatty acids were then extracted using 2 mL isooctane. The remaining lipids solutions were centrifuged 5 minutes at 2000 rpm at 25 °C to obtain a tri-phasic separation. The supernatant organic phase was removed. This step was performed three times. Dried samples were diluted in 100 µL isooctane for gas chromatography. The PL concentration (nmol/mL) was then normalized over the implant surface (nmol/mL/mm²).

3. Results

3.1. Tissue analysis

The general appearance of the sample harvested from the different cases is shown in the supplementary materials for each staining and immunostaining (figures S1 to S5). Details are provided below.

- CrCo

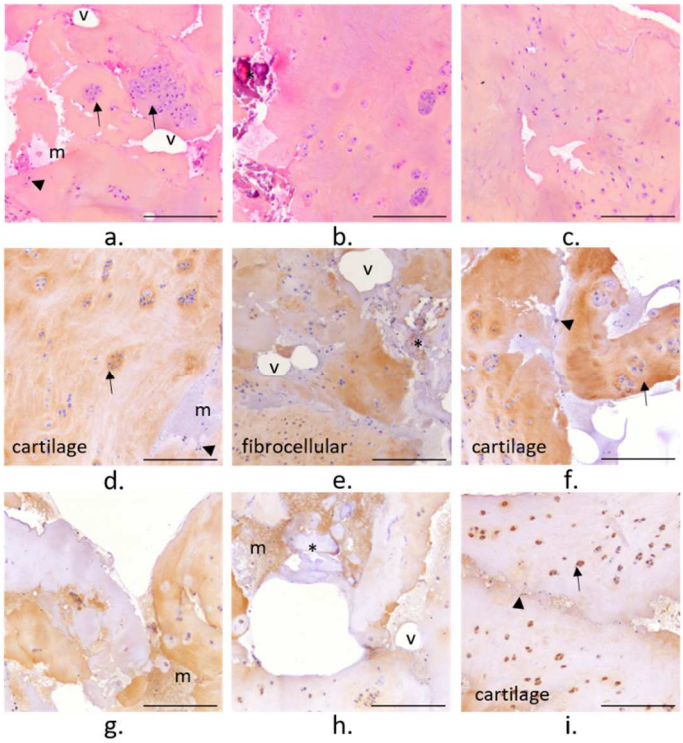

Figure 2: Histological microscopic images of the membrane harvested from the case with the CrCo head. a/b/c: HES, d/e/f: Coll I, g/h/i: Coll II; m: bone marrow; v: vascular canal; □: chondrocytes; *: mineralized area; ►: black particles. Scale bar = 200 µm. column fitting image

The membrane harvested from the clinical case 1 with an implanted CrCo head appeared as a loose and multi-layered tissue (Figure S1). The tissue presented areas with hypertrophic chondrocytes (➔). Large clusters of these chondrocytes were also observed. Large areas of low cell density were observed. Some mineralized areas were observed (*, Figure 2b, e, and h) together with a bone marrow or haemorrhagic type matrix (m). Sparse black particles were also observed over the membrane (►, Figure 2a, f, and i). Coll I was more expressed over the membrane compared to Coll II. The areas with chondrocytes or chondrocytes clusters were mainly composed of Coll I, suggesting that the tissue is mainly a fibrocartilaginous tissue. Still, some Coll II was expressed intracellularly. The tissue was highly vascularized all over the sample (v) (Figure 2).

The bone core harvested from the CrCo case presented a porous bone network (Figure S2). Bone marrow was characterized as a dense and hypercellular marrow (m)(Bartl, 2013) that presented a fibrocellular in some area with a high expression of Col l, highlighting an inflammation of the marrow (Figure 4). Granulation tissue was also observed in the bone marrow (Figure 4b).

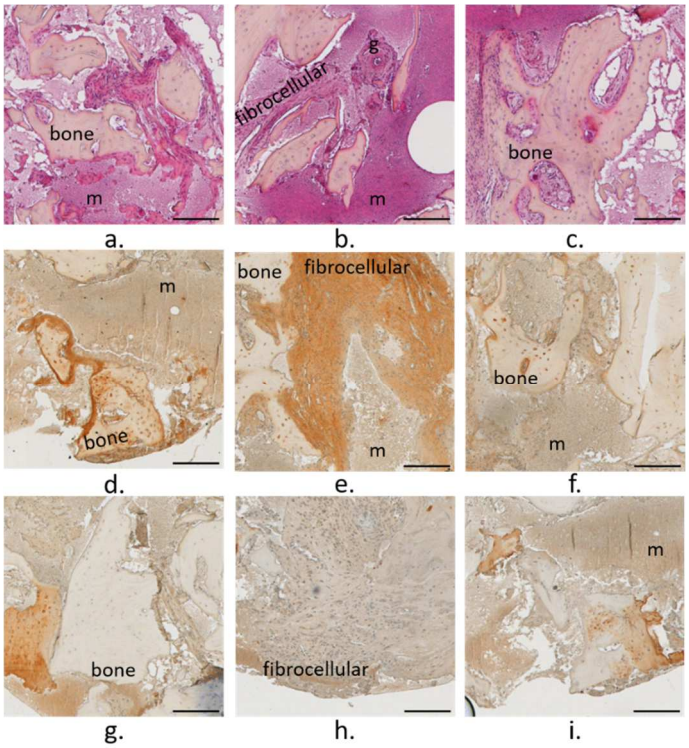

Figure 4: Histological microscopic images of the bone core harvested from the case with the CrCo head. a/b/c: HES, d/e/f: Coll I, g/h/i: Coll II; m: bone marrow; v: vascular canal; g: granulation tissue. Scale bar = 200 µm. 1 column fitting image

158 • PyC

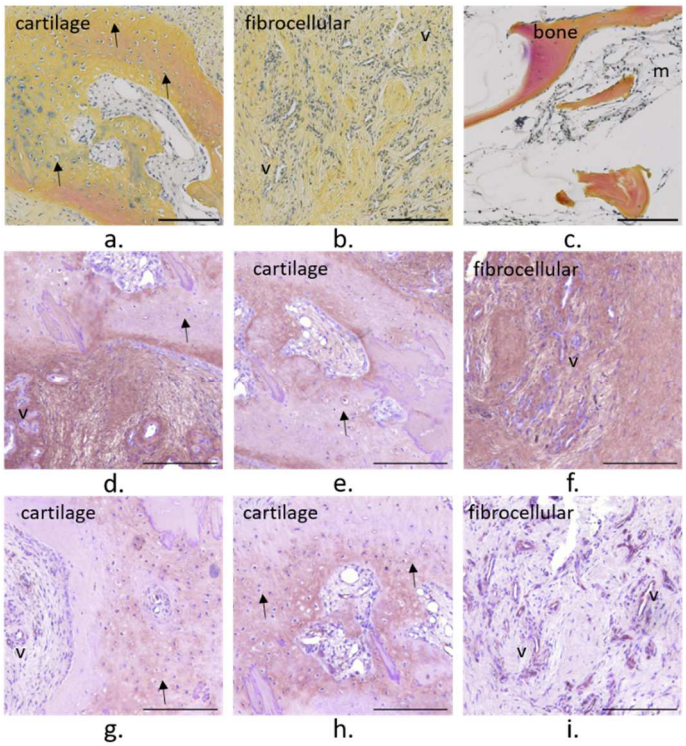

Figure 3: Histological microscopic images of the bone-cartilage core harvested from the case with the PyC head. a/b/c: HES, d/e/f: Coll I, g/h/i: Coll II; m: bone marrow; v: vascular canal; ➔: chondrocytes. Scale bar = 200 µm. 1 column fitting image

The membrane harvested from the clinical case 2 with a PyC head but no microdrilling appeared as a thick and dense membrane (Figure S3). The tissue was mainly made of a fibrocellular and vascularized tissue (v) mainly composed of Coll I. Still an amorphous region filled with chondrocytes (➔, Figure 3a) and composed of Coll II (Figure 3g, and h) highlighted the presence of an articular cartilage-like tissue. It has to be noticed that Coll II was expressed on the vascular canals surface (Figure 3). The bone marrow (m) appeared less dense than for the previous case. But unfortunately, the core harvested by the surgeon did not presented a large quantity of bone tissue.

- µPyC

The membrane harvested from the clinical case 3 with a PyC head and subchondral microdrills appeared as a dense a thick membrane (Figure S4). The tissue presented an area of fibrocellular tissue surrounded by cartilaginous tissue. The tissue on the bone side appeared vascularized (v) whereas on the implant side a cartilaginous tissue with chondrocytes (➔) was observed (Figure 5). Still on the implant side, a dense layer highlight expressed in Coll II was observed ({). Coll I and II were expressed intensively in different areas, and also within the chondrocytes pericellular matrices (Figure 5e, h, and i). Clusters of two chondrocytes oriented perpendicularly to the membrane surface were observed (Figure 5e and h). Coll II was expressed on the vascular canal surfaces (Figure 5i).

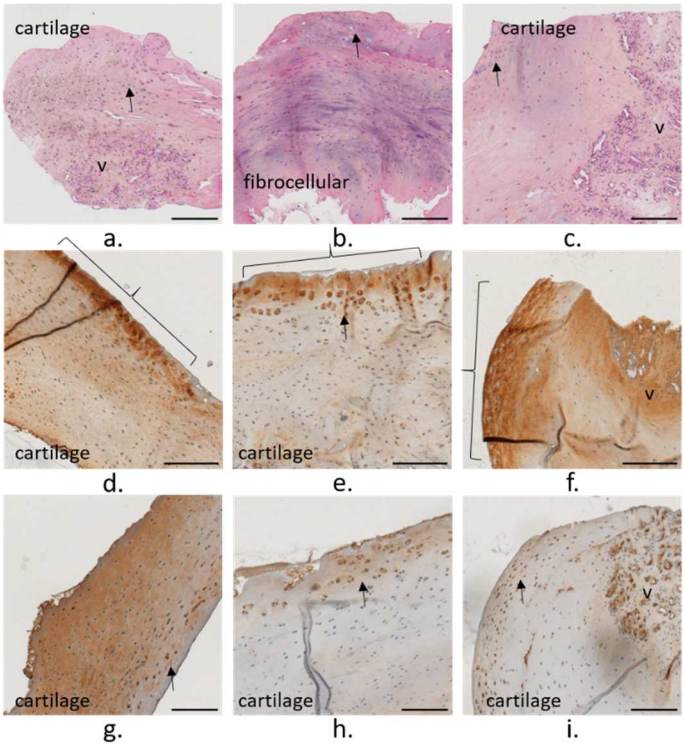

Figure 5: Histological microscopic images of the membrane harvested from the case with the PyC head with subchondral microdrills. a/b/c: HES, d/e/f: Coll I, g/h/i: Coll II; v: vascular canal; □: chondrocytes. Scale bar = 200 µm. 1 column fitting image

The bone core presented a more compact region on the implant side and a porous one away from the implant (Figure S5). A low-density bone marrow (m) was observed with some sparse region of fibrocellular matrix (Figure 6). Coll I was mainly expressed in the bone marrow, and Coll II was expressed on the surface of vascular canals (v) (Figure 6h and i).

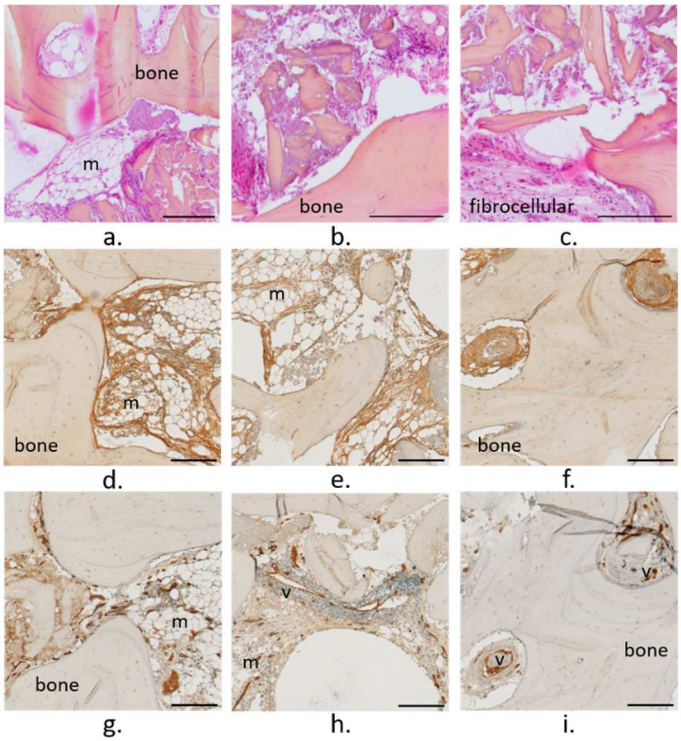

Figure 6: Histological microscopic images of the bone core harvested from the case with the PyC head with subchondral microdrills. a/b/c: HES, d/e/f: Coll I, g/h/i: Coll II; m: bone marrow; v: vascular canal. Scale bar = 200 µm. 1 column fitting image

3.2. Lipidomic analysis

The concentration of phospholipids (PL) extracted from the hemi-implant heads was lower on the CrCo head compared to the PyC, with a higher concentration obtained on the µPyC head after microdrilling in the subchondral bone (Figure 7).

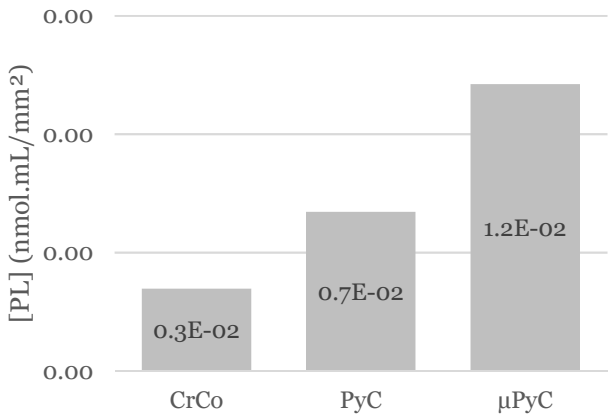

Figure 7: Phospholipids concentration normalized by the surface of each hemi-implant head ([PL] in nmol/mL/mm²). 1 column fitting image

4. Discussion

Shoulder hemi-arthroplasty (HA) currently represents an interesting way to maintain the mobility for the treatment of osteoarthritis or humeral trauma. Still, the complex frictional interaction between the hemi-implant head and the native glenoid cavity may result in glenoid erosion, decreasing the patient quality of life and increasing the risk for the implant revision. In the current study, the glenoid tissues

(cartilage and bone) harvested from three clinical cases that underwent different natures of HA (CrCo head, PyC head, and PyC head with subchondral microdrills) were characterized through histology. The results showed that the nature of the glenoid tissues depended on the nature of the HA protocol. The case with the CrCo head presented the worst tissue. On the other hand, the case with the PyC head and subchondral microdrills appeared as the best case.

While the membrane harvested from the CrCo case presented a large area of cartilage, this cartilage was of bad quality, as highlighted by the presence of large clusters of chondrocytes (Lotz et al., 2010) and of acellular areas (Lotz and Loeser, 2012). Furthermore, the membrane was mainly composed of Coll I, that is not a biomarker for an healthy articular cartilage, but more of a fibrocartilaginous tissue (Benjamin and Evans, 1990). The presence of haemorrhagic areas supported the inflammation of this glenoid cartilage membrane.

In contrast, a region of articular-like cartilage was observed on the membrane harvested from the PyC case. Even if this region was surrounded by a vascularized fibrocellular tissue, the formed cartilage in this membrane was of good quality according to this histological analysis. It is also interesting to observed Coll II on the vascular canals surface. Coll II, synthetized by the chondrocytes, is a biomarker for articular cartilage. Observing Coll II in the vascular network suggests that the suitable biological signal for articular cartilage synthesis has been sent to the vascularized subchondral bone.

In the µPyC case, the tissue looked like an articular cartilaginous-like tissue, except for a vascularized area and a fibrocellular region on the bone side. The dense layer on the implant sided reminded of the dense layer on the cartilage surface (Sophia Fox et al., 2009), supporting a good sliding interactions between the PyC implant on the glenoid cartilage membrane (Sakai et al., 2016).

It is interesting to see that the nature of these different glenoid cartilage membranes was in accordance with the features observed in the bone cores, more particularly in the bone marrow. The hypercellular and fibrous tissue observed for the CrCo case support an inflammatory state of the bone marrow. Furthermore, the granulation tissue is also in accordance with a degenerative cartilage (Bogoch et al., 2007). Conversely, the morphology of the bone marrow observed in the µPyC case is more representative of a healthy state of the subchondral bone (Bogoch et al., 2007). It is also interesting to observed the expression of Coll II in the bone marrow for the µPyC, suggesting that a chondrogenesis signalling was transmitted to the chondrogenic bone marrow cells (Li et al., 2009). Unfortunately, only a small part of bone is seen on the bone-cartilage core harvested from the PyC case. Still, the small region of bone marrow presented a morphology closer to that from the µPyC case.

Bone marrow lesions are known to be associated with cartilage degeneration, reflecting the damaged state of the subchondral bone (Alliston et al., 2018). Hence, these results strongly suggest the influence of the hemi-implant material and the HA procedure on the biomechanical loading transmitted to the subchondral bone. This hypothesis is further supported by the lipidomic analyses showing a higher amount of PL adsorbed to the PyC surface compare to the CrCo. This results is in accordance with previous *ex vivo* analyses showing a better adsorption of PL on PyC during friction on cartilage (Impergre et al., 2023). Similar to the native cartilage, this higher concentration of PL may decrease the friction interactions between the PyC and the native glenoid tissues. This in turns decrease the frictional forces and promote the sliding between the PyC implant and the native cavity. In addition to an improve mechanobiological behaviour of the implanted joint, a decrease frictional force may also prevent from implant particles to be released in the contacting tissue, as it was observed in the tissue harvested from the CrCo case. The PyC better capacity to adsorbed a layer of PL may explain the better clinical outcomes obtained with PyC HA compared to CrCo HA.

Interestingly, the concentration of PL on the µPyC with subchondral microdrills was higher than the PyC alone. This supports the liberation of PL from the bone marrow and their diffusion toward the implant surface. Hence, in addition to the releasing of chondrogenic stem cells from the bone marrow, microdrills may also improve the biomechanical interactions within the implanted joint.

This study is limited by a low number of cases, with 1 case per HA configuration. It has to be noticed that PyC has only recently been used for shoulder HA (McBride et al., 2021) and the number of PyC HA revision remains low. The current study has been initiated in the 2015's by our groups after the observation of a neosynthtized cartilaginous like tissue at the bone-pyrocarbon interface by orthopaedic surgeons. A large collection of these tissue explanted at the time of a PyC HA revision is undergoing. The current study supports the relevance of such collection to better understand the influence of PyC on the integrity of the glenoid cartilage. More particularly, the current study strongly suggest that the PyC is able to send a suitable signal to the subchondral bone to promote cartilage integrity regulation. Amongst others, this signalling seems to be sent with the suitable biomechanical configuration offered by the couple PyC – phospholipids, promoting the lubrication of the PyC glenoid cavity lubrication (Figure 8).

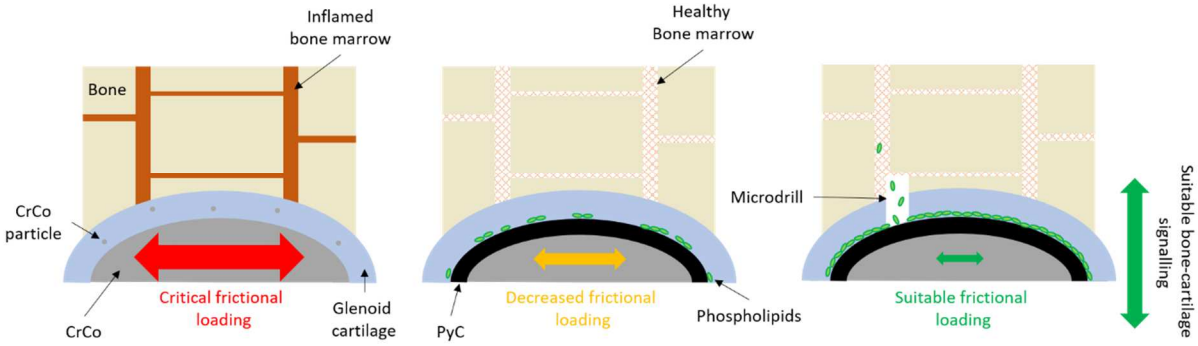

Figure 8: Schematic of the implanted glenoid cavity and the hypothesized difference between the three investigated clinical cases. 2 columns fitting image

5. Conclusion

In the current study, the glenoid cartilage and bone harvested from 3 clinical cases who underwent three different shoulder hemi-arthroplasties: a case with a cobalt-chrome head, a second with a pyrocarbon head, and a last with a pyrocarbon head and subchondral microdrills. The histological and lipidomic analyses showed better quality cartilage and bone tissues of better quality for the pyrocarbon head with subchondral microdrills. Pyrocarbon capacity to adsorb a phospholipids layer on its surface associated with the liberation of bone marrow phospholipids through the microdrills may improve the biomechanical interactions at the cartilage implant interface. Despite the limitations of this study, the results obtained strongly support the interest to further analyse the pyrocarbon glenoid cavity biomechanical interactions to better understand the implanted joint integrity and the tissue quality at the hemi implant interface. The aim is to enhance patients' quality of life, avoid should hemi-implant failure and revision.

6. Conflict of interest

Amira Hanoun and Michel Hassler are employed by Tornier SAS that commercialize the pyrocarbon hemi implant investigated in the current study. These authors, their immediate family, and any research foundation with which they are affiliated did not receive any financial payments or other benefits from any commercial entity related to the subject of this article. The other authors declare no conflict of interest.

7. Acknowledgements

This study was funded by Tornier SAS. The authors wish to thanks Dr. Olivier Menouillard (Ramsay Santé, Höpital privé Pays de Savoie, Annemasse, France), Dr. Arnaud Godenèche (Hôpital privé Jean Mermoz Ramsay-GDS, Centre Orthopédique Santy, Lyon, France), and Dr Robert Hudek (Klinik für

Schulter- und Ellbogenchirurgie, RHÖN KlinikumAG, Bad Neustadt, Germany) for the tissue samples and the clinical data about the three cases investigated in the current study.

8. References

Alliston, T., Hernandez, C.J., Findlay, D.M., Felson, D.T., Kennedy, O.D., 2018. Bone marrow lesions in osteoarthritis: What lies beneath. J. Orthop. Res. 36, 1818–1825. https://doi.org/10.1002/jor.23844

Bartl, R., 2013. Histology of Normal Bone and Bone Marrow, and Their Main Disorders. pp. 3–20. https://doi.org/10.1007/174_2011_442

Benjamin, M., Evans, E.J., 1990. Fibrocartilage. J. Anat. 171, 1–15. https://doi.org/10.1007/978-1-4939-3305-1_5

Bogoch, E.R., Lee, T.C., Fornasier, V.L., Berger, S.A., 2007. Articular damage is associated with intraosseous inflammation in the subchondral bone marrow of joints affected by experimental inflammatory arthritis and is modified by zoledronate treatment. J. Rheumatol. 34, 1229–1240.

Broyles, J.E., O'Brien, M.A., Stagg, M.P., 2017. Microdrilling Surgery Augmented With Intra-articular Bone Marrow Aspirate Concentrate, Platelet-Rich Plasma, and Hyaluronic Acid: A Technique for Cartilage Repair in the Knee. Arthrosc. Tech. 6, e201–e206. https://doi.org/10.1016/J.EATS.2016.09.024

Chan, S.M.T., Neu, C.P., Komvopoulos, K., Reddi, A.H., Di Cesare, P.E., 2011. Friction and Wear of Hemiarthroplasty Biomaterials in Reciprocating Sliding Contact With Articular Cartilage. J. Tribol. 133. https://doi.org/10.1115/1.4004760

Coughlin, T.R., Kennedy, O.D., 2016. The role of subchondral bone damage in post-traumatic osteoarthritis. Ann. N. Y. Acad. Sci. 1383, 58–66. https://doi.org/10.1111/nyas.13261

During, A., Penel, G., Hardouin, P., 2015. Understanding the local actions of lipids in bone physiology. Prog. Lipid Res. https://doi.org/10.1016/j.plipres.2015.06.002

Elder, S.H., Cooley, A.J., Borazjani, A., Sowell, B.L., To, H., Tran, S.C., 2009. Production of hyaline-like cartilage by bone marrow mesenchymal stem cells in a self-assembly model. Tissue Eng. - Part A 15, 3025–3036. https://doi.org/10.1089/ten.tea.2008.0617

Franceschetti, E., Gregori, P., Giurazza, G., Papalia, G., Caraffa, A., Papalia, R., 2023. Short to Early-Mid Term Clinical Outcomes and Survival of PyrocarbonShoulder Implants: A Systematic Review and Meta-Analysis. J. Shoulder Elb. Arthroplast. 7, 247154922311521. https://doi.org/10.1177/24715492231152143

Garret, J., Harly, E., Le Huec, J.-C., Brunner, U., Rotini, R., Godenèche, A., 2019. Pyrolytic carbon humeral head in hemi-shoulder arthroplasty: preliminary results at 2-year follow-up. JSES Open Access 3, 37–42. https://doi.org/10.1016/j.jses.2018.09.002

Hills, B.A., 2002. Surface-active phospholipid: A Pandora's box of clinical applications. Part II. Barrier and lubricating properties. Intern. Med. J. 32, 242–251. https://doi.org/10.1046/j.1445-5994.2002.00201.x

Impergre, A., Trunfio-Sfarghiu, A.-M., Wimmer, M.A., 2023. Evaluation of articular cartilage wear against pyrolytic carbon in the context of spherical interposition shoulder arthroplasty. Biotribology 33–34, 100237. https://doi.org/10.1016/j.biotri.2023.100237

Klawitter, J.J., Patton, J., More, R., Peter, N., Podnos, E., Ross, M., 2020. In vitro comparison of wear characteristics of PyroCarbon and metal on bone: Shoulder hemiarthroplasty. Shoulder Elb. 12, 11–22. https://doi.org/10.1177/1758573218796837

Levine, W.N., Fischer, C.R., Nguyen, D., Flatow, E.L., Ahmad, C.S., Bigliani, L.U., 2012. Long-Term Follow-up of Shoulder Hemiarthroplasty for Glenohumeral Osteoarthritis. J. Bone Jt. Surg. 94, e164-1–7. https://doi.org/10.2106/JBJS.K.00603

Li, Z., Yao, S.J., Alini, M., Stoddart, M., 2009. Chondrogenesis of human bone marrow mesenchymal stem cells is modulated by frequency and amplitude of dynamic compression and shear stress. Eur. Cells Mater. 18, 51. https://doi.org/10.1089=ten.tea.2009.0262

Lotz, M.K., Loeser, R.F., 2012. Effects of aging on articular cartilage homeostasis. Bone 51, 241–248. https://doi.org/10.1016/j.bone.2012.03.023

Lotz, M.K., Otsuki, S., Grogan, S.P., Sah, R., Terkeltaub, R., D'Lima, D., 2010. Cartilage cell clusters. Arthritis Rheum. 62, 2206–2218. https://doi.org/10.1002/art.27528

Martin, R., Jakob, R.P., 2022. Review of K.H. Pridie (1959) on "A method of resurfacing osteoarthritic knee joints." J. ISAKOS 7, 39–46. https://doi.org/10.1016/J.JISAKO.2021.11.001

Matsen, F.A., Clinton, J., Lynch, J., Bertelsen, A., Richardson, M.L., 2008. Glenoid component failure in total shoulder arthroplasty. J. Bone Jt. Surg. - Ser. A 90, 885–896. https://doi.org/10.2106/JBJS.G.01263

McBride, A.P., Ross, M., Hoy, G., Duke, P., Page, R., Peng, Y., Taylor, F., 2021. Mid-term outcomes of pyrocarbon humeral resurfacing hemiarthroplasty compared to metal humeral resurfacing and metal stemmed hemiarthroplasty for osteoarthritis in young patients: Analysis from the Australian Orthopaedic Association National Joint Replace. J. Shoulder Elb. Surg. https://doi.org/10.1016/j.jse.2021.08.017

Papadonikolakis, A., Neradilek, M.B., Matsen, F.A., 2013. Failure of the Glenoid Component in Anatomic Total Shoulder Arthroplasty. J. Bone Jt. Surg. 95, 2205–2212. https://doi.org/10.2106/jbjs.l.00552

Sakai, N., Hashimoto, C., Yarimitsu, S., Sawae, Y., Komori, M., Murakami, T., 2016. A functional effect of the superficial mechanical properties of articular cartilage as a load bearing system in a sliding condition. Biosurface and Biotribology 2, 26–39. https://doi.org/10.1016/J.BSBT.2016.02.004

Sophia Fox, A.J., Bedi, A., Rodeo, S.A., 2009. The Basic Science of Articular Cartilage: Structure, Composition, and Function. Sport. Heal. A Multidiscip. Approach 1, 461–468. https://doi.org/10.1177/1941738109350438

Vanlommel, J., De Corte, R., Luyckx, J.P., Anderson, M., Labey, L., Bellemans, J., 2017. Articulation of Native Cartilage Against Different Femoral Component Materials. Oxidized Zirconium Damages Cartilage Less Than Cobalt-Chrome. J. Arthroplasty 32, 256–262. https://doi.org/10.1016/j.arth.2016.06.024

Zarka, M., Hay, E., Ostertag, A., Marty, C., Chappard, C., Oudet, F., Engelke, K., Laredo, J.D., Cohen-Solal, M., 2019. Microcracks in subchondral bone plate is linked to less cartilage damage. Bone 123, 1–7. https://doi.org/10.1016/J.BONE.2019.03.011